6. COMPARISONS AND CONCLUSION

6.1. INTRODUCTION

Voltage controlled buses need special consideration in the load flow solution methods as the ability of these buses to maintain constant voltage is dependent upon the availability of reactive resources. Conventional load flow methods handle the problem by forcing the reactive power to the limiting values whenever the calculated reactive power at the buses exceeds their limits. Evolutionary load flows proposed in the thesis handle the voltage-controlled buses in a very similar way. The method followed being the same for all the evolutionary algorithms, is discussed in the present chapter.

Handling of FACTS devices needs special mention because of the control functions to be performed by the FACTS devices and the speciality of the variables involved. This chapter also discusses the handling of the FACTS devices in the evolutionary algorithms which also is same for all the algorithms developed.

Finally a comparative analysis of the performance of different evolutionary load flows is made, the achievements and shortcomings of the thesis are highlighted and the scope of future research has been identified.

6.2. CONSIDERATION OF THE VOLTAGE CONTROLLED BUSES

Voltage controlled buses do not require any special treatment in the proposed load flows. The treatment here is very similar to the conventional load flow analysis. If the computed reactive power of the voltage controlled bus is within the reactive power limits, voltage magnitude is kept at the specified value and is not calculated using the proposed technique. If, however, the calculated reactive power is outside the given range, its reactive power mismatch is calculated with respect to the limiting values and voltage magnitude is calculated using normal PSO technique. Thus, if Q-limits are not violated, voltages remain fixed at specified values. On the other hand, if the limits are violated reactive powers are automatically enforced at the limiting values.

To check the Q-limit of the generator buses, the following steps mentioned in Fig. 6.1 are used.

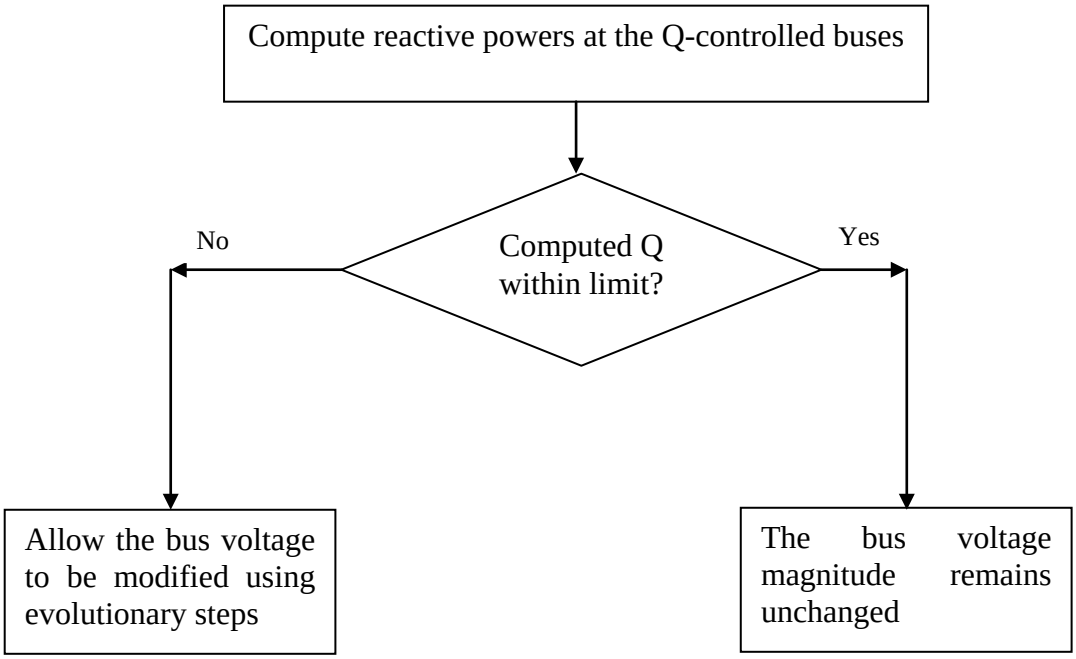

Fig. 6.1: Steps for Q-limit checking

6.3. APPLICATION OF THE FACTS DEVICES

Flexible alternating current transmission system (FACTS) devices are used for the dynamic control of voltage, impedance and phase angle of high voltage AC line. FACTS devices provide strategic benefits for improved transmission system management through better utilization of existing transmission assets; increased Transmission system reliability and availability; increased dynamic and transient grid stability and increased quality of supply for sensitive industries (e.g. computer chip manufacture).

Unified Power Flow Controller (UPFC) is the most versatile among all types of FACTS devices. UPFCs can be used for voltage as well as power flow control. Handling of the UPFC in the evolutionary load flows is discussed in this section. Fig. 6.2 shows the equivalent circuit of UPFC.

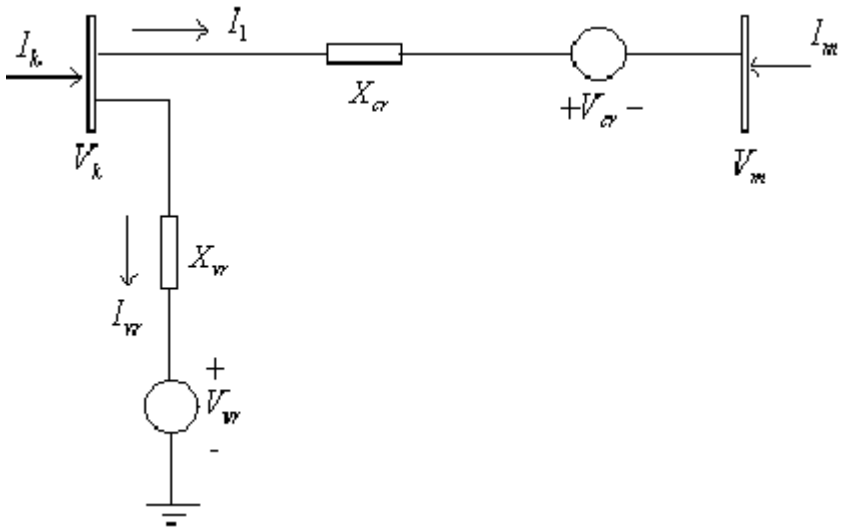

Fig. 6.2: UPFC equivalent circuit

The equivalent circuit consists of two ideal voltage sources representing the fundamental Fourier series component of the switched voltage waveforms at the AC converter terminals. The ideal voltages sources are:

$$V_{vR} = V_{vR} (\cos\theta_{vR} + j \sin\theta_{vR}) \quad (6.1)$$

$$V_{cR} = V_{cR} (\cos\theta_{cR} + j \sin\theta_{cR}) \quad (6.2)$$

Where V_{vR} and θ_{vR} are the controllable magnitude ($V_{vRmin} \leq V_{vR} \leq V_{vRmax}$) and angle ($0 \leq \theta_{vR} \leq 2\pi$) of the voltage source representing the shunt converter. The magnitude V_{cR} and angle θ_{cR} of the voltage source of the series converter are controlled between limits ($V_{cRmin} \leq V_{cR} \leq V_{cRmax}$) and ($0 \leq \theta_{cR} \leq 2\pi$), respectively.

6.3.1. UPFC POWER EQUATIONS

Based on the equivalent circuit shown in Fig. 6.1, the active and reactive power equations can be written as:

At node k:

$$P_k = V_k^2 G_{kk} + V_k V_m (G_{km} \cos(\theta_k - \theta_m) + B_{km} \sin(\theta_k - \theta_m))$$
$$+ V_k V_{cR} (G_{km} \cos(\theta_k - \theta_{cR}) + B_{km} \sin(\theta_k - \theta_{cR}))$$
$$+ V_k V_{vR} (G_{vR} \cos(\theta_k - \theta_{vR}) + B_{vR} \sin(\theta_k - \theta_{vR})) \quad (6.3)$$

$$Q_k = - V_k^2 B_{kk} + V_k V_m (G_{km} \sin(\theta_k - \theta_m) - B_{km} \cos(\theta_k - \theta_m))$$

$$+ V_k V_{cR} (G_{km} \sin(\theta_k - \theta_{cR}) - B_{km} \cos(\theta_k - \theta_{cR}))$$
$$+ V_k V_{vR} (G_{vR} \sin(\theta_k - \theta_{vR}) - B_{vR} \cos(\theta_k - \theta_{vR})) \quad (6.4)$$

At node m:

$$P_m = V_m^2 G_{mm} + V_m V_k (G_{mk} \cos(\theta_m - \theta_k) + B_{mk} \sin(\theta_m - \theta_k))$$
$$+ V_m V_{cR} (G_{mm} \cos(\theta_m - \theta_{cR}) + B_{mm} \sin(\theta_m - \theta_{cR})) \quad (6.5)$$

$$Q_m = - V_m^2 B_{mm} + V_m V_k (G_{mk} \sin(\theta_m - \theta_k) - B_{mk} \cos(\theta_m - \theta_k))$$
$$+ V_m V_{cR} (G_{mm} \sin(\theta_m - \theta_{cR}) - B_{mm} \cos(\theta_m - \theta_{cR})) \quad (6.6)$$

Series converter:

$$P_{cR} = V_{cR}^2 G_{mm} + V_{cR} V_k (G_{km} \cos(\theta_{cR} - \theta_k) + B_{km} \sin(\theta_{cR} - \theta_k))$$
$$+ V_{cR} V_m (G_{mm} \cos(\theta_{cR} - \theta_m) + B_{mm} \sin(\theta_{cR} - \theta_m)) \quad (6.7)$$

$$Q_{cR} = - V_{cR}^2 B_{mm} + V_{cR} V_k (G_{km} \sin(\theta_{cR} - \theta_k) - B_{km} \cos(\theta_{cR} - \theta_k))$$
$$+ V_{cR} V_m (G_{mm} \sin(\theta_{cR} - \theta_m) - B_{mm} \cos(\theta_{cR} - \theta_m)) \quad (6.8)$$

Shunt converter:

$$P_{vR} = -V_{vR}^2 G_{vR} + V_{vR} V_k (G_{vR} \cos(\theta_{vR} - \theta_k) + B_{vR} \sin(\theta_{vR} - \theta_k)) \quad (6.9)$$

$$Q_{vR} = V_{vR}^2 B_{vR} + V_{vR} V_k (G_{vR} \sin(\theta_{vR} - \theta_k) - B_{vR} \cos(\theta_{vR} - \theta_k)) \quad (6.10)$$

where,

$$Y_{kk} = G_{kk} + jB_{kk} = z_{cR}^{-1} + z_{vR}^{-1} \quad (6.11)$$
$$Y_{mm} = G_{mm} + jB_{mm} = z_{cR}^{-1} \quad (6.12)$$
$$Y_{km} = Y_{km} = G_{km} + jB_{km} = -z_{cR}^{-1} \quad (6.13)$$
$$Y_{vR} = G_{vR} + jB_{vR} = -z_{vR}^{-1} \quad (6.14)$$

6.3.2. IMPLEMENTATION OF THE FACTS DEVICES

Two methods have been developed for inclusion of UPFC in the load flow problem. In the first method, an estimate of the UPFC variables is first calculated using the UPFC power settings and the system bus voltages. One set of such estimates is computed for each string of the solution population. These solutions are then updated using evolutionary technique. The steps to obtain the UPFC variables are given in Fig. 6.3.

Initial estimates of the UPFC variables are computed as [13]:

$$\theta_{cr}^{o} = \arctan\left(\frac{P_{mref}}{|D|}\right) \tag{6.15}$$

$$V_{cr}^{o} = \frac{X_{cr}}{V_{m}^{o}}\sqrt{P_{mref}^{2} + D^{2}} \tag{6.16}$$

$$D = Q_{mref} - \frac{V_m}{X_{cr}}(V_m - V_k) \tag{6.17}$$

$$\theta_{vr}^{o} = -\arcsin\left(\frac{(V_k^{o} - V_m^{o})V_{cr}^{o}X_{vr}\sin(\theta_{cr}^{o})}{V_{vr}^{o}V_k^{o}X_{cr}}\right) \tag{6.18}$$

X_{cr}, X_{vr} are the series and shunt inductive reactance. Superscript $'o'$ is used to indicate initial value.

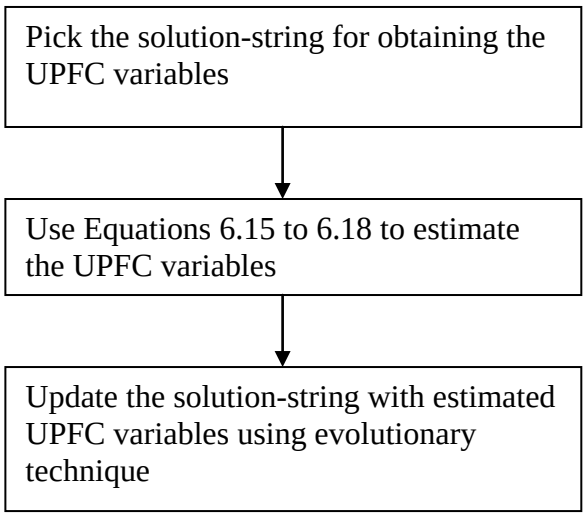

Fig. 6.3: Initial estimation of the UPFC variables

In the second approach, for each string of the solution population, starting values for the UPFC variables are first estimated. A population of solution strings for the UPFC is then initialized around the starting values of the variables. These solution populations are then iterated using evolutionary technique and the best solution is determined. This process is repeated for each solution string of the normal load flow. The steps to evaluate the best UPFC variables are shown in Fig. 6.4.

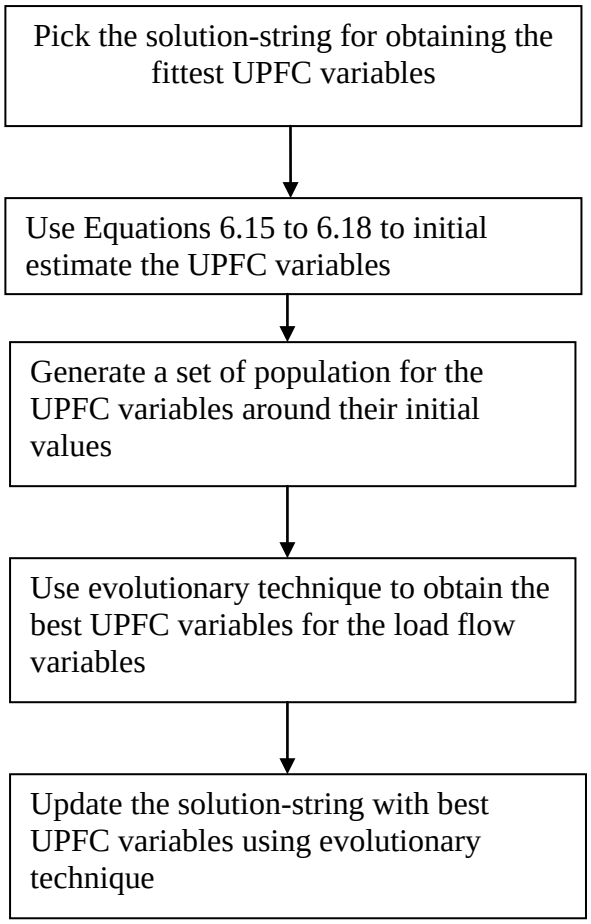

Fig. 6.4: Steps to get best UPFC variables

6.3.3. LOAD FLOW RESULTS WITH THE FACTS DEVICES

The developed methods have been tested by incorporating UPFCs in the standard test systems and convergence achieved for all the experiments performed. However, the number of generations required for solution increases after UPFC is incorporated. Of the two schemes described above, the second one takes lesser number of iterations. Some of the results obtained for the modified IEEE-14 Bus test system with a UPFC included to control the power flow through the line connected between buses 14 and 13 are presented here. A new bus 15 had to be created to facilitate the connection of the UPFC that is included between buses 14 & 15. While UPFC has been modeled to keep the voltage of bus 14 fixed at 1.0 p.u., active and reactive power flows through the line are varied in a wide range as given in Table 6.3, where the corresponding voltages and phase angles for the whole systems are also presented. Table 6.4 shows the values of the UPFC variables for the respective cases.

Table 6.3
Results obtained by the Proposed Method with Different Power Settings

Line Flow in p.u.	Results (Voltage Magnitude in p.u. & Phase angle in degree)
-0.0558-0.0158j	V=[1.0600 1.0450 1.0100 1.0160 1.0180 1.0700 1.0560 1.0900 1.0450 1.0420 1.0524 1.0417 1.0244 1.0000 0.9846] Delta=[0 -5.1313 -12.9695 -10.6052 -9.0813 -15.1197 -13.7957 -13.7957 -15.4635 -15.6863 -15.5266 -15.9131 -15.6273 -16.1927 -17.1657]
-0.3918-0.3518j	V=[1.0600 1.0450 1.0100 1.0093 1.0105 1.0700 1.0551 1.0900 1.0483 1.0448 1.0539 1.0407 1.0172 1.0000 0.7380] Delta=[0 -6.1778 -14.7063 -12.8303 -11.1700 -20.0957 -17.5276 -17.5276 -19.9584 -20.2663 -20.3032 -21.6338 -22.0911 -24.0006 -29.9286]
0.1144+0.1544j	V=[1.0600 1.0450 1.0100 1.0181 1.0205 1.0700 1.0559 1.0900 1.0433 1.0405 1.0515 1.0419 1.0269 1.0000 1.0685] Delta=[0 -4.7403 -12.3216 -9.7688 -8.2953 -13.2508 -12.3944 -12.3944 -13.7724 -13.9636 -13.7308 -13.7570 -13.1852 -13.2321 -12.5123]

Table 6.4
UPFC variables for test cases

Line Flow in p.u / FACTS Parameters	-0.0558-0.0158j	-0.3918-0.3518j	0.1144+0.1544j
V_{vr} in p.u.	0.9501	0.9000	1.1000
V_{cr} in p.u.	0.0058	0.0530	0.0193
θ_{cr} in degree	-73.7576	-47.4366	36.7413
θ_{vr} in degree	-16.1850	-23.4002	-13.1847

6.4 TIME COMPARISON OF THE EVOLUTIONARY TECHNIQUES

The author proposed three population based load flow such as PSO based coupled algorithm, PSO based decoupled algorithm and Two-stage GA based load flows. For different size of population, the convergence-time of PSO based coupled algorithm without and with the improvement schemes are given in Table 6.5 and Table 6.6 respectively. The program developed and run on Pentium IV CPU 2.40 GHz, 256 MB of RAM, 40 GB hard disc computer using MATLAB version.

Table 6.5
Time comparison of PSO based coupled algorithm

Test Systems	IEEE 30 bus		IEEE 57 bus		IEEE 118 bus	
Size of population	100	1000	100	1000	100	1000
Total number of generation	998	48	1419	73	2232	224
Time per generation in sec.	2.4690	24.2030	6.1090	61.3120	17.8120	180.1064
Total time in sec.	2464.1	1161.7	8668.7	4475.8	39756.4	40344.6

Table 6.6
Time comparison of PSO based coupled algorithm with Local Search

Test Systems	IEEE 30 bus			IEEE 57 bus			IEEE 118 bus		
Size of population	100	20	12	100	20	12	100	20	12
Total number of generation	22	51	92	31	69	132	42	84	198
Time per generation in sec.	3.0150	1.0780	0.8900	9.4530	3.6250	3.1410	45.8750	21.8440	20.4380
Total time in sec.	66.3300	54.9780	81.8800	293.0430	250.1250	414.6120	1926.8	1834.9	4046.7

If the updated scheme is used with the PSO based coupled algorithm, then time per generation becomes more than the coupled algorithm without improvement scheme. But total convergence-time is 40-times less for coupled algorithm with improvement scheme. Time comparison of PSO based decoupled algorithm without and with improvement schemes are shown in Table 6.7 and Table 6.8 respectively.

Table 6.7
Time comparison of PSO based decoupled algorithm

Test Systems	IEEE 30 bus		IEEE 57 bus		IEEE 118 bus	
Size of population	100	04	100	04	100	04
Total number of generation	102	152	141	224	213	327
Time per generation in sec.	3.5470	0.1870	9.3280	0.4370	25.5150	1.2030
Total time in sec.	361.7940	28.4240	1315.2	97.8880	5434.7	393.3810

Table 6.8
Time comparison of PSO based decoupled algorithm with Local Search

Test Systems	IEEE 30 bus		IEEE 57 bus		IEEE 118 bus	
Size of population	10	02	10	02	10	02
Total number of generation	30	44	43	59	72	92
Time per generation in sec.	0.7350	0.4680	3.8090	1.3420	17.8120	4.2190
Total time in sec.	22.0500	20.5920	163.7870	79.1780	1282.5	388.1480

The solution-time decreases like coupled algorithm if improvement scheme is used with the decoupled algorithm. For decoupled algorithm, total convergence-time and time per generation are much less than the coupled algorithm. For different size of population, comparisons of convergence-time of two-stage GA based load flow without and with the advancement scheme have been given in fig. Table 6.9 and Table 6.10 respectively.

Table 6.9
Time comparison of Two Stage GA based load flow

Test Systems	IEEE 30 bus			IEEE 57 bus			IEEE 118 bus		
Size of population	100	10	08	100	10	08	100	10	08
Total number of generation	196	303	598	258	472	763	404	798	1012
Time per generation in sec.	79.8130	8.0310	6.0250	554.9370	55.4690	44.0470	3988.0	398.7350	323.2190
Total time in sec.	15643.8	2433.4	3961.8	143173.7	26181.4	33608.1	1611152.0	318190.5	327097.6

Table 6.10
Time comparison of Two Stage GA with Local Search based load flow

Test Systems	IEEE 30 bus			IEEE 57 bus			IEEE 118 bus		
Size of population	10	08	04	10	08	04	10	08	04
Total number of generation	92	111	523	118	132	811	169	184	1083
Time per generation in sec.	12.3910	9.3130	4.3600	76.0470	64.2660	32.1410	596.0310	415.8900	260.9680
Total time in sec.	1139.9720	1033.7430	2280.2800	8973.5460	8483.1120	26066.3510	100729.2390	76523.7600	282628.344

In case of two-stage GA based load flow with the improvement scheme, Time per generation is approximately 1.5 times greater than the proposed method without improvement scheme. But total convergence-time for the developed method without improvement scheme is almost 3-times more than the developed method with improvement scheme.

For the population based load flows the best time comparisons have been given in Table 6.11 and Table 6.12 shows best time comparisons among the population based load flow methods with Local Search.

Table 6.11
Best time (in sec.) Comparisons among the population based load flow methods

Test Systems	IEEE 30 bus	IEEE 57 bus	IEEE 118 bus
Coupled PSO method	1161.7	4475.8	40344.7
Decoupled PSO method	28.424	97.888	393.381
Two stage GA method	2433.4	26181.8	318190.6

Table 6.12
Best time (in sec.) Comparisons among the population based load flow methods with Local Search

Test Systems	IEEE 30 bus	IEEE 57 bus	IEEE 118 bus
Coupled PSO method	54.9780	250.1250	1834.9
Decoupled PSO method	20.5920	79.1780	388.1480
Two stage GA method	1033.7430	8483.1120	76523.7600

In two-Stage GA method, number of generation decreases with the increase of population size but according to convergence time best results is obtained with a population size of 10. This method cannot give good results below 10 population size whereas PSO algorithm based decoupling method gives best results with the population size as low as 4. PSO algorithm based on variable coupling method is the simplest method and shows best results at very high population size as per both performance index and convergence time. With the help of Local Search both the convergence time and number of generation have been improved significantly. Among the three population based power flow methods Decoupled based PSO method shows the best results from every respect like convergence time, number of generation.

6.5 PERFORMANCE UNDER CRITICAL CONDITIONS

All the methods proposed in the thesis showed convergence without failure for all types of ill conditioning. This has been tested by increasing the loading of the test systems upto their maximum loading conditions and the results have been verified with those obtained from continuation power flow [14]. The load multipliers (by which system base loads were multiplied) for which a solution can be obtained are shown in Table 6.13 for different test systems. Load flow solution for the maximum permissible loading of 3.0686 times the standard values for IEEE 30 bus system are produced in Table 6.14. Robustness of the algorithms has also been tested by varying the line R/X ratios. For this purpose line resistances and reactances are multiplied by values greater than 1 and less than 1 respectively as reported in [8] and the results are produced in Table 6.15 and Table 6.16.

Table 6.13
Load Multipliers for the Maximum Loading Conditions

Test System	5-bus	IEEE 14-bus	IEEE 30-bus	IEEE 57-bus	IEEE 118-bus
Newton Raphson	3.0361	4.0078	3.0523	1.7916	2.0392
Proposed power flows	3.0887	4.0115	3.0686	1.8103	2.0469

Table 6.14
Results for IEEE 30 Bus System With the Load Multiplied by 3.0686

V=[1.0500 1.0338 0.9198 0.9163 1.0058 0.9416 0.9372 1.0230 0.9154 0.8334 1.0913
0.9109 1.0883 0.8447 0.8189 0.8505 0.8178 0.7725 0.7582 0.7733 0.7781 0.7789
0.7583 0.7128 0.6967 0.6070 0.7314 0.9196 0.6036 0.5287] in p.u.

Delta=[0 -21.7036 -28.3500 -34.7155 -51.2568 -40.8691 -47.0055 -44.0203 -51.8412
-59.7652 -49.7041 -57.6453 -56.2702 -61.5758 -61.7935 -59.7079 -60.7507 -64.6583
-65.4146 -64.2286 -62.1086 -62.0571 -63.6499 -64.4176 -64.2458 -67.3340 -62.4753
-42.8401 -71.2129 -79.6641] in degrees

Table 6.15
Line Resistance Multiplier for the Critical Cases

Test System	5-bus	IEEE 14-bus	IEEE 30-BUS	IEEE 57-bus	IEEE 118-bus
Newton Raphson	7.1658	4.4222	5.1211	4.4101	5.0704
Proposed power flows	7.1764	4.4371	5.1304	4.4252	5.0732

Table 6.16
Line Reactance Multiplier for the Critical Cases

Test System	IEEE 14-bus	IEEE 30-bus	IEEE 57-bus	IEEE 118-bus
Newton Raphson	0.0491	0.0554	0.0655	0.0696
Proposed power flows	0.0419	0.0401	0.0588	0.0624

From the above test results it has been observed that the proposed methods give better performances under critical conditions. All the developed methods show their robustness, efficiency and non-diverging characteristics for each type of critical condition.

6.6 CONCLUSION

Heuristic and Evolutionary techniques have been used to develop a number of load flow methods in the present thesis. All these load flows are rugged and can be used for solving ill conditioning problems including the problem of the determination of the loadability limit. The proposed load flows clearly can not compete with the popular load flow methods in terms of solution speed. But in critical situations when conventional ones fail, the proposed load flows undoubtedly will be the choice. Besides the development of the load flow algorithms, the present thesis has also made an effort to study the applicability of the evolutionary techniques in solving the load flow problem. Among the evolutionary techniques the PSO seems to be more appropriate for the load flow problem. While the PSO based decoupled

algorithm perform better in obtaining normal solution, the algorithm where the coupling between the power system variables are retained are efficient in finding the multiple load flow solutions.

The contribution of the author in the present thesis may be summarized as follows:

i. Development of a local network based load flow
ii. Development of linear perturbation based load flow
iii. Application of the PSO algorithm in developing a decoupled load flow algorithm
iv. Application of the PSO algorithm in developing load flow for finding multiple solutions
v. Development of two-stage GA based load flow

6.7 SHORTCOMING OF THE REPORTED WORKS

Tap changing transformer ratio and shunt capacitor taps have not been considered as variables in the implementations of the proposed load flows. These variables are to be modeled for constrained power flow analysis. Constrained power flow may prove to be a very useful tool for the operation of power systems in the new market environment.

6.8 SCOPE OF FUTURE RESEARCH

The developed evolutionary load flows may be modified with the little efforts to solve constrained power flow problem. Such modifications will help further researches on the operation and control of deregulated power system.

Multiple power flow solutions give useful information regarding the voltage stability of power system. The PSO based power flow thus may help further research on voltage stability.

Population based power flows along with the conventional Newton-Raphson power flows have been used in the present work to generate the PV-QV curves. The author feels that perturbation based power flow alone, with certain modifications, will be able to solve continuous of power flows. The perturbation based power flow thus may be made to work as a continuation power flow method.

6.9 DATA AND RESULTS

6.9.1. STAGG 5-BUS SYSTEM DATA

6.9.1.1. Line Data of 5-bus test system

Line No	Start Bus	End Bus	R	X	Ysh	Tap set
1	1	2	0.0200	0.0600	0.0600	1.0000
2	1	3	0.0800	0.2400	0.0500	1.0000
3	2	3	0.0600	0.1800	0.0400	1.0000
4	2	4	0.0600	0.1800	0.0400	1.0000
5	2	5	0.0400	0.1200	0.0300	1.0000
6	3	4	0.0100	0.0300	0.0200	1.0000
7	4	5	0.0800	0.2400	0.0500	1.0000

6.9.1.2 Bus Data of 5-bus test system

Bus No	Pgen	Qgen	Pload	Qload	Vm	Delta	Bus code	Ysh_c	Qmin	Qmax
1	0	0	0	0	1.0600	0	1.0000	0	0	0
2	0.4000	0.3000	0.2000	0.1000	1.0000	0	0	0	0	0
3	0	0	0.4500	0.1500	1.0000	0	0	0	0	0
4	0	0	0.4000	0.0500	1.0000	0	0	0	0	0
5	0	0	0.6000	0.1000	1.0000	0	0	0	0	0

6.9.1.3. Network Diagram of Stagg-5 Bus System

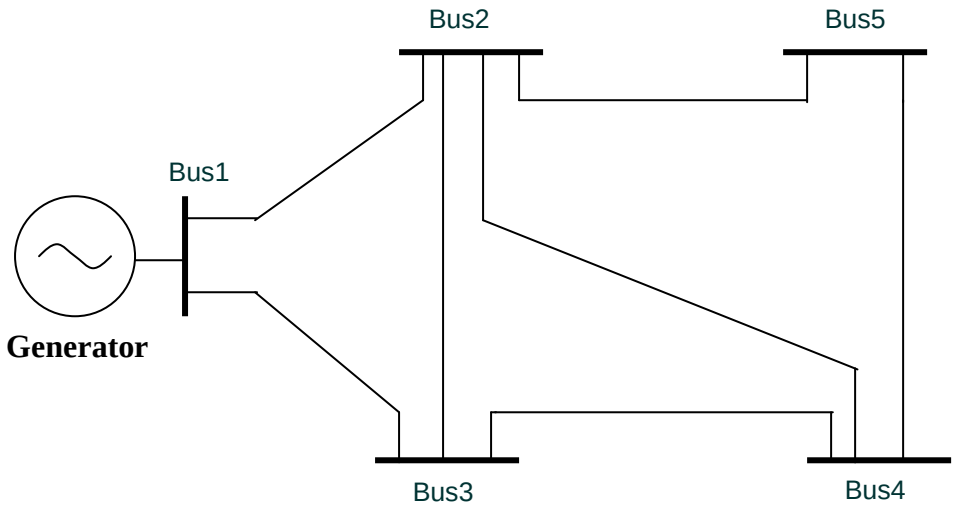

6.9.2. IEEE 14-BUS SYSTEM DATA

6.9.2.1. Line Data of 14-bus test system

Line No	Start Bus	End Bus	R	X	Ysh	Tap set
1	1	2	0.0194	0.0592	0.0264	1.0000
2	2	3	0.0470	0.1980	0.0219	1.0000
3	2	4	0.0581	0.1763	0.0187	1.0000
4	1	5	0.0540	0.2230	0.0246	1.0000
5	2	5	0.0570	0.1739	0.0170	1.0000
6	3	4	0.0670	0.1710	0.0173	1.0000
7	4	5	0.0134	0.0421	0.0064	1.0000
8	5	6	0	0.2520	0	0.9320
9	4	7	0	0.2091	0	0.9780
10	7	8	0	0.1762	0	1.0000
11	4	9	0	0.5562	0	0.9690
12	7	9	0	0.1100	0	1.0000
13	9	10	0.0318	0.0845	0	1.0000
14	6	11	0.0950	0.1989	0	1.0000
15	6	12	0.1229	0.2558	0	1.0000
16	6	13	0.0662	0.1303	0	1.0000
17	9	14	0.1271	0.2704	0	1.0000
18	10	11	0.0820	0.1921	0	1.0000
19	12	13	0.2209	0.1999	0	1.0000
20	13	14	0.1709	0.3480	0	1.0000

6.9.2.2 Bus Data of 14-bus test system

Bus No	Pgen	Qgen	Pload	Qload	Vm	Delta	Bus code	Ysh_c	Qmin	Qmax
1	0	0	0	0	1.0600	0	1.0000	0	0	0
2	0.4000	0	0.2170	0.1270	1.0450	0	2.0000	0	-0.400	0.5000
3	0	0	0.9420	0.1900	1.0100	0	2.0000	0	0	0.4000
4	0	0	0.4780	0.0400	1.0000	0	0	0	0	0
5	0	0	0.0760	0.0160	1.0000	0	0	0	0	0
6	0	0	0.1120	0.0750	1.0700	0	2.0000	0	-0.060	0.2400
7	0	0	0	0	1.0000	0	0	0	0	0
8	0	0	0	0	1.0900	0	2.0000	0	-0.060	0.2400
9	0	0	0.2950	0.1660	1.0000	0	0	0.1900	0	0
10	0	0	0.0900	0.0580	1.0000	0	0	0	0	0
11	0	0	0.0350	0.0180	1.0000	0	0	0	0	0
12	0	0	0.0610	0.0160	1.0000	0	0	0	0	0
13	0	0	0.1350	0.0580	1.0000	0	0	0	0	0
14	0	0	0.1490	0.0500	1.0000	0	0	0	0	0

6.9.2.3. Network Diagram of IEEE-14 Bus System

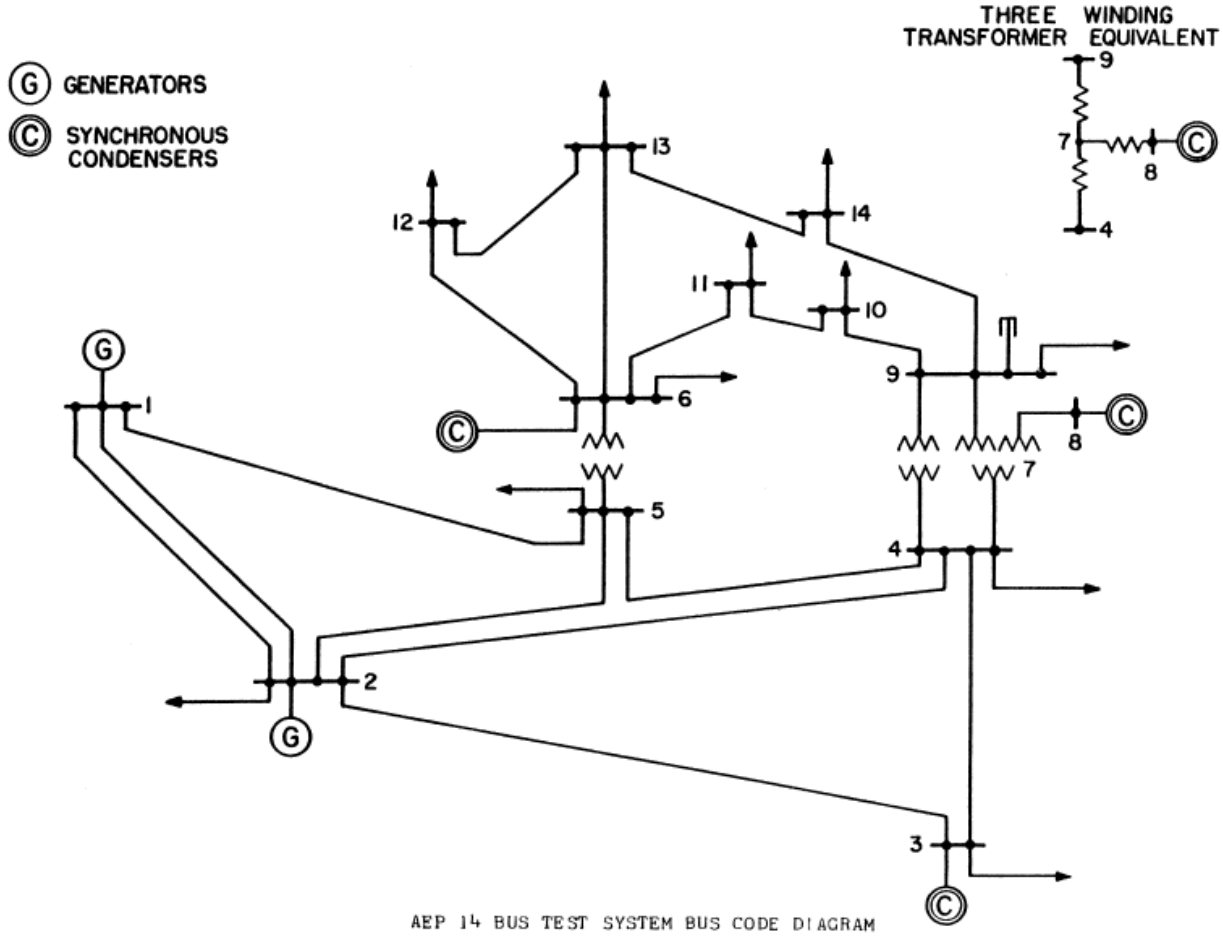

6.9.3. IEEE 30- BUS SYSTEM DATA

6.9.3.1. Line Data of 30-bus test system

Line No	Start Bus	End Bus	R	X	Ysh	Tap set
1	1	2	0.0192	0.0575	0.0264	1.0000
2	1	3	0.0452	0.1852	0.0204	1.0000
3	2	4	0.0570	0.1737	0.0184	1.0000
4	3	4	0.0132	0.0379	0.0042	1.0000
5	2	5	0.0472	0.1983	0.0209	1.0000
6	2	6	0.0581	0.1763	0.0187	1.0000
7	4	6	0.0119	0.0414	0.0045	1.0000
8	5	7	0.0460	0.1160	0.0102	1.0000
9	6	7	0.0267	0.0820	0.0085	1.0000
10	6	8	0.0120	0.0420	0.0045	1.0000
11	6	9	0	0.2080	0	1.0155
12	6	10	0	0.5560	0	0.9629
13	9	11	0	0.2080	0	1.0000
14	9	10	0	0.1100	0	1.0000
15	4	12	0	0.2560	0	1.0129
16	12	13	0	0.1400	0	1.0000
17	12	14	0.1231	0.2559	0	1.0000
18	12	15	0.0662	0.1304	0	1.0000
19	12	16	0.0945	0.1987	0	1.0000
20	14	15	0.2210	0.1997	0	1.0000
21	16	17	0.0824	0.1932	0	1.0000
22	15	18	0.1070	0.2185	0	1.0000
23	18	19	0.0639	0.1292	0	1.0000
24	19	20	0.0340	0.0680	0	1.0000
25	10	20	0.0936	0.2090	0	1.0000
26	10	17	0.0324	0.0845	0	1.0000
27	10	21	0.0348	0.0749	0	1.0000
28	10	22	0.0727	0.1499	0	1.0000
29	21	22	0.0116	0.0236	0	1.0000
30	15	23	0.1000	0.2020	0	1.0000
31	22	24	0.1150	0.1790	0	1.0000
32	23	24	0.1320	0.2700	0	1.0000
33	24	25	0.1885	0.3292	0	1.0000
34	25	26	0.2544	0.3800	0	1.0000
35	25	27	0.1093	0.2087	0	1.0000
36	28	27	0	0.3960	0	0.9581
37	27	29	0.2198	0.4153	0	1.0000
38	27	30	0.3202	0.6027	0	1.0000
39	29	30	0.2399	0.4533	0	1.0000
40	8	28	0.0636	0.2000	0.0214	1.0000
41	6.	28	0.0169	0.0599	0.0065	1.0000

6.9.3.2 Bus Data of 30-bus test system

Bus No	Pgen	Qgen	Pload	Qload	Vm	Delta	Bus code	Ysh_c	Qmin	Qmax
1	0	0	0	0	1.0500	0	1.0000	0	-0.2000	0.6000
2	0.5756	0	0.2170	0.1270	1.0338	0	2.0000	0	-0.4000	0.6000
3	0	0	0.0240	0.0120	1.0000	0	0	0	0	0
4	0	0	0.0760	0.0160	1.0000	0	0	0	0	0
5	0.2456	0	0.9420	0.1900	1.0058	0	2.0000	0	-0.1500	0.6250
6	0	0	0	0	1.0000	0	0	0	0	0
7	0	0	0.2280	0.1090	1.0000	0	0	0	0	0
8	0.3500	0	0.3000	0.3000	1.0230	0	2.0000	0	-0.1500	0.5000
9	0	0	0	0	1.0000	0	0	0	0	0
10	0	0	0.0580	0.0200	1.0000	0	0	0.1900	0	0
11	0.1793	0	0	0	1.0913	0	2.0000	0	-0.1000	0.4000
12	0	0	0.1120	0.0750	1.0000	0	0	0	0	0
13	0.1691	0	0	0	1.0883	0	2.0000	0	-0.1500	0.4500
14	0	0	0.0620	0.0160	1.0000	0	0	0	0	0
15	0	0	0.0820	0.0250	1.0000	0	0	0	0	0
16	0	0	0.0350	0.0180	1.0000	0	0	0	0	0
17	0	0	0.0900	0.0580	1.0000	0	0	0	0	0
18	0	0	0.0320	0.0090	1.0000	0	0	0	0	0
19	0	0	0.0950	0.0340	1.0000	0	0	0	0	0
20	0	0	0.0220	0.0070	1.0000	0	0	0	0	0
21	0	0	0.1750	0.1120	1.0000	0	0	0	0	0
22	0	0	0	0	1.0000	0	0	0	0	0
23	0	0	0.0320	0.0160	1.0000	0	0	0	0	0
24	0	0	0.0870	0.0670	1.0000	0	0	0.0400	0	0
25	0	0	0	0	1.0000	0	0	0	0	0
26	0	0	0.0350	0.0230	1.0000	0	0	0	0	0
27	0	0	0	0	1.0000	0	0	0	0	0
28	0	0	0	0	1.0000	0	0	0	0	0
29	0	0	0.0240	0.0090	1.0000	0	0	0	0	0
30	0	0	0.1060	0.0190	1.0000	0	0	0	0	0

6.3.9.3. Network Diagram of IEEE-30 Bus System